

Excited state nonlinear optics of quasi one-dimensional Mott-Hubbard insulators

Haranath Ghosh*

Max Planck Institute for the Physics of Complex Systems, Nöthnitzer StraÙ 38, 01187 Dresden, Germany.

(Dated: March 4, 2007)

Ground as well as excited state non-linear optical properties of one-dimensional Mott-Hubbard insulators are discussed in details. One dimensional strongly correlated materials are predicted to have several orders-of-magnitude larger *excited state* optical non-linearities in comparison to that from the ground state. Unlike π -conjugated polymers and other classes of one dimensional systems, strongly correlated materials like Sr_2CuO_3 , halogen bridged *Ni* compounds etc. have excited one- and two-photon allowed states almost energetically degenerate which leads to order(s)-of-magnitude larger dipole coupling between them in comparison to that between the ground and optical state. This causes several orders-of-magnitude enhancement in the optical non-linearities obtained from the first two-photon state in the wavelength region suitable for terahertz communications. Our results and conclusions are based on exact numerical calculations of extended Hubbard model suitable strongly correlated systems. We argue based on theoretical as well as available experimental data that one-dimensional cuprates would be good source of terahertz radiation, to be experimentally verified. We also discuss in detail ground state non-linear properties like third-harmonic generation, two-photon absorption, electro-absorption from the theoretical model and compare with experiments. Theoretical calculations of excited state nonlinearities of some π -conjugated polymers are also presented for comparison.

PACS numbers: 71.27.+a, 78.20Bh, 78.47.+p, 42.65.-k

I. INTRODUCTION

Electron-electron correlation in condensed matter systems exhibited a large number of wonders like superconductivity, magnetism, giant magneto resistence and many others [1]; enhanced optical non-linearity is also proved to be the manifestations of strong coulomb repulsion among conducting electrons together with quantum confinement [2-5]. Research on nonlinear optics of strongly correlated one dimensional systems were originated from [2, 3], both of which principally showed the occurrence of nearly degenerate one- and two-photon states due to strong coulomb correlation. These nearly degenerate one- and two-photon states are also strongly dipole coupled. This was also the reason for strong optical non-linearity obtained through two photon absorption (TPA), electroreflectance spectra of these compounds, and analysed theoretically. Spin-charge separation on Sr_2CuO_3 system [4, 6-8], joint influence of charge transfer gap and on-site [5] repulsion was emphasised. Potential of Sr_2CuO_3 single crystals as a non-linear optical material for all optical switching devices was pointed out [9]. Similarly for Halogen-bridged Nickel chain compounds ultrafast optical switching to a metallic state by photoinduced Mott- transition was reported [10]. Further important developments like evidence of two types of charge transfer excitations in Sr_2CuO_3 was found from electron energy-loss spectroscopy analysis [11]. Higher dimen-

sional counter parts of these materials (*e.g.*, $\text{Sr}_2\text{CuO}_2\text{Cl}_2$) are found to have an order of magnitude lower optical non-linearity [12, 14, 21]. Even then such stimulating science and application research in one-dimension has also lead to the study of non-linear optical properties in higher dimensional Mott-Hubbard systems [13] too. Furthermore, femtosecond spectroscopic studies in quasi-two dimensional cuprates [13] revealed strong role played by magnetic excitations in ultrafast non-radiative relaxation processes, which is related to the large Heissenberg exchanges in cuprates.

Subsequently, large third-order optical non-linearity in one dimensional Cu - O chain systems like Sr_2CuO_3 , Ca_2CuO_3 were investigated by third harmonic generation (THG) spectroscopy [15], some of these results were reconfirmed by A. Maeda *et al.*, [16] by Z-scan technique and by M. Ono *et al.*, [17] alongwith detailed studies on Ni-Halogen chain compounds. There are some discrepancies in these studies too which we discuss later. One dominant one photon peak at $\omega_A = 0.61$ eV, a two photon resonant peak $\omega_B = 0.87$ eV were observed together with an *oscillatory structure* at $\omega_C \sim 2 \times \omega_B$ and $\omega_A \simeq 2\omega_B/3$, in case of Sr_2CuO_3 . Thus the one-photon state is at energy $0.61 \times 3 = 1.83$ eV whereas the two-photon state at $0.87 \times 2 = 1.74$ eV — the two-photon state is below the one-photon state. This observation is contrary to the other earlier studies, the two-photon state is above the one-photon state [2, 3]. We shall show that this energy ordering of low energy excited states is extremely significant for photoinduced absorption (PA), excited state optical nonlinearities etc. Furthermore, determination of locations of one- and two-photon states obtained in [3] by three-level system fitting procedure seems to be doubtful because we shall show that the concerned two-photon state corresponds to the dip of the

*On leave from: Laser Physics Application Division, Raja Ramanna Centre for Advanced Technology, Indore - 452013, India.
hng@mpipks-dresden.mpg.de

$\text{Im } \chi^{(3)}(-\omega; 0, 0, \omega)$. On the contrary, locations of two-photon states in [3, 17] appears to be away from the dip of $\text{Im } \chi^{(3)}(-\omega; 0, 0, \omega)$. This would lead to the fact that the energy difference between the one- and two-photon states would be even smaller than predicted and might be reversed ordered as well similar to the observation in [15]. These would further shed light on the mechanism of gigantic non-linearities in these materials.

In this paper, one of our prime interests are theoretical prediction of huge *excited state* optical non-linearities compared to that from the ground state in these classes of materials. Here first, we theoretically demonstrate the observed THG spectrum and that the *oscillatory structure* at ω_C is another higher energy two-photon state which can be verified experimentally. We also present TPA, EA, PA theoretically and compare with available experimental data. These results of ground state non-linear as well as linear properties compare excellently well with experiments. Then we consider the case of third-order nonlinear optical susceptibilities from an excited state rather than the ground state to predict a general enhancement [18] in 1-d Mott-Hubbard insulators. We predict from our theoretical calculation that these classes of materials would have *several orders-of-magnitude larger* excited state optical non-linearities (*e.g.*, excited state-THG, -TPA, -EA) compared to that from the ground state. We emphasize this is an artifact of strongly correlated nature of these systems — π -conjugated polymers can also have about two orders of magnitude larger excited state optical non-linearity compared to that of the ground state. So far it was well known that π -conjugated organic molecules and polymer systems are of interest due to the delocalized π -electron systems which give rise to large values of $\chi^{(3)}$ but one dimensional Mott-Hubbard systems on the contrary are not so delocalized but dominated by electron-electron repulsion. Furthermore, choice of large optical non-linear medium depends not only on the ground state but also the excited states matter [20]. Nonlinear optical materials with large third-order nonlinear susceptibilities, fast response time, low loss and operability at room temperature are indispensable for next generation all-optical switching, computing devices, because the magnitude of this quantity strongly influences on the instrument performance. One of the pioneering experimental demonstration of excited state enhancement of optical nonlinearities was by Rodenberger *et al.*, in linear conjugated molecules [18] showing around two orders of magnitude enhancement in non-linearity. 50 to 160 fold increase in third order non-linearity was also observed in bacteriochlorophylls [19]. However, there are no studies yet on excited state non-linearities on one dimensional Mott-Hubbard insulators (as mentioned earlier) and given earlier experimental demonstrations in π -conjugated organic molecules [18, 19] we hope experimental verification of our theoretical predictions will also be possible. We also predict that at least one dimensional Cu-O chain systems may be used as a source for terahertz radiation (THz) source. This is because the lowest

2-ph electronic state is below 1-ph state and energetically degenerate.

Rest of the paper is organized as follows. In section II we describe a short method of numerical calculation of extended Hubbard model suitable for Mott-Hubbard systems. In section III we present detailed results of ground state linear as well as non-linear optical properties. In section IV excited state non-linear properties are discussed and its general enhancement mechanism. A short discussion on phenyl based π -conjugated polymers are also presented in this section. Detailed summary of all results and conclusions are drawn in the V-th section.

II. THEORETICAL MODEL CALCULATION

One of the most widely used theoretical model for studying strongly correlated electron system is known as Hubbard model. One dimensional Mott-Hubbard insulators that we are concerned about are Sr_2CuO_3 , Ca_2CuO_3 and $[\text{Ni}(\text{chxn})_2\text{X}]\text{Y}_2$ where $X \equiv$ Halogen (like Cl, Br etc.), $\text{chxn} \equiv$ cyclohexanediamine and $Y \equiv$ counter ion like Cl, Br, NO_3 . One dimensional Cu – O chains are composed of CuO_4 quadrilateral structures with shared corner oxygens, in which the Cu ion is divalent (spin quantum number $S = 1/2$) and one unpaired electron exists in the overlap of the p_x, p_y orbitals of O and the $d_{x^2-y^2}$ orbitals of Cu. Because of large on-site Coulomb repulsion energy U_{Cu} (described below) acting on Cu ions, the Mott-Hubbard gap is opened in the Cu $3d_{x^2-y^2}$ band. The occupied O 2p band is located between the Cu 3d upper Hubbard band and Cu 3d lower Hubbard band. Similarly, in case of halogen bridged Ni-Halides, Ni^{3+} ions and X^- are arranged alternately along the chain axis, forming purely 1D electronic state composed of the p_z orbitals of X and the d_{z^2} orbitals of the Ni. Four N atoms of amino groups in two chxn molecules coordinate a Ni^{3+} ion in a plane normal to the chain axis, and produce a strong ligand field. A Ni^{3+} ion is therefore in a low-spin state (d^7 ; $S = 1/2$) and one unpaired electron exists in the d_{z^2} orbital. Thus both the cuprates as well as the halogen bridged Ni compounds described above are one dimensional Mott-Hubbard insulators (involving two different kinds of bands $\text{Cu}(\text{Ni})-3d_{x^2-y^2}(3d_{z^2})$ and $\text{O}(\text{X})-2p_{x,y}(2p_z)$). Therefore, we use two band extended Hubbard model corresponding to Cu $-3d_{x^2-y^2}$ (Ni $-3d_{z^2}$) and O- $p_{x,y}(X - p_z)$ as below.

$$H = \sum_{\langle ij \rangle, \sigma} t_{ij} (c_{i\sigma}^\dagger c_{j\sigma} + h.c) + \sum_{i\sigma} (-1)^i \epsilon n_i + \sum_i U_i n_{i\uparrow} n_{i\downarrow} + \sum_i V n_i n_{i+1} \quad (1)$$

The first term of the above equation represents hopping probability between Cu(Ni) and O(X) sites, the 2nd term the on-site energies of the Cu(Ni) and O(X) and thereby defining the charge transfer energy $2\epsilon = \epsilon_{\text{O}(X)} - \epsilon_{\text{Cu}(\text{Ni})}$. The third term represents the most dominant term in the

Hamiltonian known as onsite coulomb repulsion, the energy felt by two electrons occupying the same Cu (Ni) -3d or O (X)- p orbital with opposite spin. The fourth term is known as intersite coulomb repulsion (V), repulsive energy felt by two electrons occupying the neighbouring Cu (Ni) and O (X) sites. We solve this Hamiltonian exactly numerically for a ring of 12 sites containing 6 Cu (Ni) and 6 O (X) sites. Within wide existing literatures for oxides we studied extensively for various combinations of a set of parameter values $|t| = 0.75 - 1.4$ eV, $U_{Cu(Ni)} = 10 - 8$ eV, $U_{O(X)} = 6 - 4$ eV, $\epsilon = 0.5 - 2.0$ eV, $V = 0.5 - 3$ eV that satisfies the well known value of the exchange integral $J \sim 2300 - 2800K$ [21] suitable for cuprates as well as Ni-Hallides.

The technique used here is an exact diagonalization method using second quantized valence bond (VB) technique originally developed by Mazumdar *et al.*, [22] and later by Ramasesha *et al.*, [23]. We follow the same notations of dixit and Mazumdar [22]. We describe briefly on the same for smaller system size that can also be solved exactly analytically. Imagine a ring of Cu-O-Cu-O in which odd- (even-) sites correspond to Cu (O) respectively. For a 4-site ring problem following configurations are possible in the even-parity subspace.

$$\begin{aligned} |\phi_{1+}\rangle &= \begin{pmatrix} 1 & 0 \\ 0 & 1 \end{pmatrix} \\ |\phi_{2+}\rangle &= \frac{1}{2} \left[\begin{pmatrix} 0 & 1 \\ 0 & 1 \end{pmatrix} + \begin{pmatrix} 1 & 0 \\ 1 & 0 \end{pmatrix} + \begin{pmatrix} 1 & 1 \\ 0 & 0 \end{pmatrix} + \begin{pmatrix} 0 & 0 \\ 1 & 1 \end{pmatrix} \right] \\ |\phi_{3+}\rangle &= \frac{1}{\sqrt{2}} \left[\begin{pmatrix} 2 & 0 \\ 0 & 0 \end{pmatrix} + \begin{pmatrix} 0 & 0 \\ 0 & 2 \end{pmatrix} \right] \\ |\phi_{4+}\rangle &= \frac{1}{\sqrt{2}} \left[\begin{pmatrix} 0 & 2 \\ 0 & 0 \end{pmatrix} + \begin{pmatrix} 0 & 0 \\ 2 & 0 \end{pmatrix} \right] \\ |\phi_{5+}\rangle &= \begin{pmatrix} 0 & 1 \\ 1 & 0 \end{pmatrix} \end{aligned}$$

Correspondingly the odd parity subspace would contain the following configurations :

$$\begin{aligned} |\phi_{1-}\rangle &= \frac{1}{2} \left[\left\{ \begin{pmatrix} 0 & 1 \\ 0 & 1 \end{pmatrix} + \begin{pmatrix} 1 & 0 \\ 1 & 0 \end{pmatrix} \right\} - \left\{ \begin{pmatrix} 1 & 1 \\ 0 & 0 \end{pmatrix} + \begin{pmatrix} 0 & 0 \\ 1 & 1 \end{pmatrix} \right\} \right] \\ |\phi_{2-}\rangle &= \frac{1}{\sqrt{2}} \left[\begin{pmatrix} 2 & 0 \\ 0 & 0 \end{pmatrix} - \begin{pmatrix} 0 & 0 \\ 0 & 2 \end{pmatrix} \right] \\ |\phi_{3-}\rangle &= \frac{1}{\sqrt{2}} \left[\begin{pmatrix} 0 & 2 \\ 0 & 0 \end{pmatrix} - \begin{pmatrix} 0 & 0 \\ 2 & 0 \end{pmatrix} \right] \\ |\phi_{4-}\rangle &= \frac{1}{2} \left[\left\{ \begin{pmatrix} 0 & 1 \\ 0 & 1 \end{pmatrix} + \begin{pmatrix} 1 & 1 \\ 0 & 0 \end{pmatrix} \right\} - \left\{ \begin{pmatrix} 1 & 0 \\ 1 & 0 \end{pmatrix} + \begin{pmatrix} 0 & 0 \\ 1 & 1 \end{pmatrix} \right\} \right] \\ |\phi_{5-}\rangle &= \frac{1}{2} \left[\left\{ \begin{pmatrix} 0 & 1 \\ 0 & 1 \end{pmatrix} + \begin{pmatrix} 0 & 0 \\ 1 & 1 \end{pmatrix} \right\} - \left\{ \begin{pmatrix} 1 & 0 \\ 1 & 0 \end{pmatrix} + \begin{pmatrix} 1 & 1 \\ 0 & 0 \end{pmatrix} \right\} \right] \end{aligned}$$

where the configurations $|\phi\rangle \equiv \begin{pmatrix} 1 & 2 \\ 3 & 4 \end{pmatrix}$ actually represents occupations in various sites (1,2,..) respectively. Thus one can solve the Hamiltonian in the respective subspace using the ansatz $\Psi_{\pm}^{\dagger} \hat{H}_{\pm} \Psi_{\pm}$ where $-\Psi_{\pm} \rangle = |(\phi_{1\pm} \phi_{2\pm} \phi_{3\pm} \phi_{4\pm} \phi_{5\pm})\rangle$. The actual wavefunctions in the \pm subspace will be given by, $\psi_1 = \sum a_{i\pm} \phi_{i\pm}$, $\psi_2 = \sum b_{i\pm} \phi_{i\pm}$, $\psi_3 = \sum c_{i\pm} \phi_{i\pm}$, $\psi_4 = \sum d_{i\pm} \phi_{i\pm}$, $\psi_5 = \sum e_{i\pm} \phi_{i\pm}$ where a_i, b_i, c_i, d_i, e_i denotes eigen functions of the \hat{H} in the respective sub-spaces. Dipolemo-

ments can be calculated then between \pm subspaces to study optical properties. Note that the configurations in the +ve subspace is connected by the current operator $\hat{j} \propto itane/\hbar \sum_l (c_{l+1}^{\dagger} c_l - c_l^{\dagger} c_{l+1})$ to the -ve subspace configurations, where 'a' and 'e' are lattice constant and electronic charge. On the other hand, configurations of the +ve subspace can be reached by operating the current operator twice on the ground state $|\phi_{1+}\rangle$. Results presented in the next section is for 12-site exact numerical solutions of Hamiltonian (1) based on the above mentioned procedure.

III. CALCULATION OF LINEAR AND NON-LINEAR OPTICAL SUSCEPTIBILITIES OF 1-D MOTT-INSULATORS

The electric field E of the incident light induces the dielectric polarization P_{ind} in a material, which is described by a power series of nonlinear optical susceptibility $\chi^{(n)}$: $P_{ind} = \epsilon_0 \sum_{n=1,2,3,4,5..} (\chi^{(n)} E^n)$. The linear susceptibility $\chi^{(1)}$ is given by,

$$\begin{aligned} \chi_{jk}^{(1)}(-\omega; \omega) &= \frac{1}{\epsilon_0 N} \frac{e^2}{\hbar} \sum_b \left\{ \frac{\mu_{0b}^j \mu_{b0}^k}{E_b - i\Gamma_b - \omega} + \frac{\mu_{0b}^k \mu_{b0}^j}{E_b + i\Gamma_b + \omega} \right\} \quad (2) \end{aligned}$$

where N is the system size, ϵ_0 is the dielectric constant, j and k are the polarization directions, $e\mu_{0b}$ is the dipole-moment between the ground state and the 1-photon allowed odd parity state, E_b, Γ_b are energies of the 1-photon states measured from the ground state and the damping factor respectively. Due to prototype one dimensional and centrosymmetric nature of Cu-O (Ni-X) network, the next higher order optical susceptibilities $\chi^{(2)}$ will be vanishingly small in these systems. The third order susceptibilities will be the lowest observable nonlinearities of interest and are expressed as [24],

$$\begin{aligned} \chi_{jklm}^{(3)}(-\omega_{\sigma}; \omega_1, \omega_2, \omega_3) &= \frac{1}{\epsilon_0 N} \frac{e^4}{3! \hbar} P \sum_{a,b,c} \frac{\mu_{0b}^j \mu_{ba}^k \mu_{ac}^l \mu_{c0}^m}{(E_b - i\Gamma_b - \omega_{\sigma})(E_a - i\Gamma_a - \omega_2 - \omega_3)(E_c - i\Gamma_c - \omega_3)} \quad (3) \end{aligned}$$

where $\omega_{\sigma} = \omega_1 + \omega_2 + \omega_3$, a and c denote even (two-photon allowed) and odd (one-photon allowed) states respectively, P represents permutations on the sums $(j, \omega_1), (k, \omega_2), (l, \omega_3)$ and (m, ω_{σ}) . In the present study $i = j = k = l = x$ is fixed, setting all the polarization directions the same along chains (Cu-O or Ni-X axis). The formal expression of the non-linear susceptibility relevant to THG studies is obtained by considering

$\omega_1 = \omega_2 = \omega_3 = \omega$ so that $\omega_\sigma = 3\omega$,

$$\chi_{THG}^{(3)}(-3\omega; \omega, \omega, \omega) = \frac{1}{\epsilon_0 N} \frac{e^4}{3! \hbar} \sum_{a,b,c} \frac{\mu_{0b}^j \mu_{ba}^k \mu_{ac}^l \mu_{c0}^m}{(E_b - i\Gamma_b - 3\omega)(E_a - i\Gamma_a - 2\omega)(E_c - i\Gamma_c - \omega)} \quad (4)$$

Similarly, the formal expression of the non-linear susceptibility relevant to TPA studies can be obtained by setting $\omega_1 = -\omega$ and $\omega_2 = \omega_3 = \omega$ as,

$$\chi_{TPA}^{(3)}(-\omega; -\omega, \omega, \omega) = \frac{1}{\epsilon_0 N} \frac{e^4}{3! \hbar} \sum_{a,b,c} \frac{\mu_{0b}^j \mu_{ba}^k \mu_{ac}^l \mu_{c0}^m}{(E_b - i\Gamma_b - \omega)(E_a - i\Gamma_a - 2\omega)(E_c - i\Gamma_c - \omega)} \quad (5)$$

We also study non-linear susceptibility relevant to Electro Absorption (EA) or d.c. kerr effect by setting $\omega_1 = \omega_2 = 0$ and $\omega_3 = -\omega$,

$$\chi_{EA}^{(3)}(-\omega; 0, 0, \omega) = \frac{1}{\epsilon_0 N} \frac{e^4}{3! \hbar} \sum_{a,b,c} \frac{\mu_{0b}^j \mu_{ba}^k \mu_{ac}^l \mu_{c0}^m}{(E_b - i\Gamma_b - \omega)(E_a - i\Gamma_a - \omega)(E_c - i\Gamma_c - \omega)} \quad (6)$$

The triple sum in $\chi^{(3)}(-3\omega; \omega, \omega, \omega)$ is over all possible even and odd parity states and all the energies are with respect to the ground state. We calculated 300 excited states, 150 each for even and odd parity states of the model Hamiltonian (1) and compute $150 \times 150 = 22500$ dipolemoments among them to evaluate various non-linear optical properties like THG, TPA etc. through the above mentioned formula. Before we talk about excited state non-linearities it is imperative to compare the available experimental data on THG, TPA and EA with our theoretical calculation.

IV. RESULTS AND DISCUSSIONS

A. Ground state optics

In this subsection our main aim is to provide conclusive evidence to the fact that there exists a higher energy two-photon state in the THG than the two-photon state close to the first one-photon state. In order to observe such higher energy two-photon state one should evaluate $\text{Im} \chi_{xxxx}^{(3)}(-\omega; \omega, -\omega, \omega)$ instead of $\text{Im} \chi_{xxxx}^{(3)}(-\omega; 0, 0, \omega)$. Such a higher energy two photon state may also be observable in photoinduced absorption (PA). Secondly, we would like to demonstrate that the observed intensity dependent refractive index (n_2) is reproduced excellently well within our theoretical calculations. Thirdly, we show that the mechanism of huge optical non-linearity is same in all the so far observed 1-d Mott-Hubbard insulator —

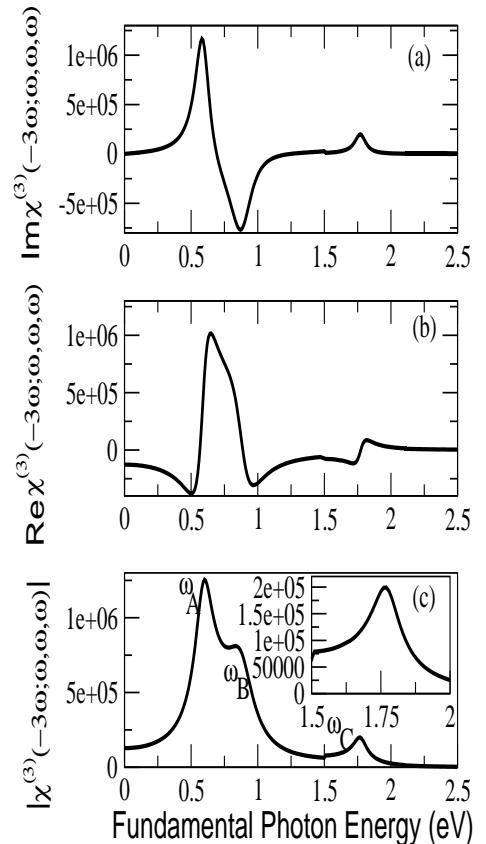


FIG. 1: Third order susceptibility of one-dimensional Mott-Hubbard insulators relevant to third harmonic generation. Imaginary part of the THG susceptibility (a), real part of the THG susceptibility (b), magnitude of the THG susceptibility (c). Locations of ω_A , ω_B , ω_C are very close to the experimentally observed values. The peak at ω_A is a three-photon resonant one whereas those at ω_B and ω_C are two-photon resonant.

it can be understood within large electron correlation, electro-negativity of lattice ions and chemical pressure.

In order to achieve our first goal of this subsection we study in detail the nature of third order susceptibility relevant for third harmonic generation (THG) explicit expressions of which are given by Eqn. (4). Parameters used in this subsection are $U_{Cu(Ni)} = 10.0$ eV, $U_{O(X)} = 6.0$ eV, $t_{Cu(Ni)-O(X)} = 1.0$ eV, $V = 0.5$ eV, $2\epsilon = 1.0$ eV, unless specified otherwise. In Fig. 1 we have shown nature of theoretically computed THG generation susceptibility expected from Hamiltonian (1) widely used for describing strongly correlated electron system. The imaginary part $\text{Im} \chi_{xxxx}^{(3)}(-3\omega; \omega, \omega, \omega)$ (Fig 1. (a)), Re

$\chi_{xxxx}^{(3)}(-3\omega; \omega, \omega, \omega)$ (Fig. 1(b)) and the magnitude which was observed experimentally [15] $|\chi_{xxxx}^{(3)}(-3\omega; \omega, \omega, \omega)| = \sqrt{(\text{Im}\chi_{xxxx}^{(3)})^2 + (\text{Re}\chi_{xxxx}^{(3)})^2}$ (Fig. 1(c)) are shown in Fig. 1 for comparison as a function of fundamental photon energy (in eV). It is evident from Fig. 1(a) and (b) that where the Im part (as a function of photon energy) rise the Re part decreases and vice-versa. This trend is also followed in Figs. 3, 4. A look into the Eqn (4) will lead to the fact that the THG susceptibility can have resonances at 3ω , 2ω corresponding to the three-photon resonant, two-photon resonant absorptions respectively as well as in ω for two-photon resonant absorptions. The nature of $|\chi_{xxxx}^{(3)}(-3\omega; \omega, \omega, \omega)|$ given in Fig. 1(c) is explainable given that the Re and Im parts are displayed in Figs. 1(a) and (b). Very low intensity but broad absorption peak at ω_C is shown pronounced in the inset figure Fig. 1(c). Given that nonlinearity in the lower frequency regime is very large the lower intensity peak at ω_C would still be observed experimentally if probed in the photon energy region as indicated in the inset Fig. 1(c). We point out that the first peak at ω_A is a three-photon resonant one whereas the peaks at ω_B and ω_C correspond to the lower and higher energy two-photon resonant absorptions respectively. In order to identify two-photon resonant absorption peaks we exhibit third order susceptibilities relevant for two-photon absorption in figures 2 and 3.

In Fig. 2 we have plotted Im and Re parts of $\chi_{xxxx}^{(3)}(-\omega; -\omega, \omega, \omega)$ whereas in Fig. 3 Im and Re parts of $\chi_{xxxx}^{(3)}(-\omega; 0, 0, \omega)$. The Im $\chi_{xxxx}^{(3)}(-\omega; -\omega, \omega, \omega)$ signifies two-photon absorption whereas the Re $\chi_{xxxx}^{(3)}(-\omega; -\omega, \omega, \omega)$ is related to the intensity dependent refractive index of a material. All optical switching devices conventionally uses the light-induced change of the refractive index n_2 rather than the two-photon absorption coefficient. Since the Re and Im parts of the $\chi_{xxxx}^{(3)}(-\omega; -\omega, \omega, \omega)$ are related by Kramers-Kronig (K-K) transformation, observed strong TPA is accompanied by large n_2 can be visualized from our theoretical calculations in Fig. 2. We would like to mention that only three experimental data points for n_2 is available [9] but our theoretical results provide possible nature of n_2 as a function of entire energy range. Our results on n_2 agrees well with K-K transformed observed TPA data ; precisely indicating large values of n_2 near optical fiber communication wavelength $1.55 \mu\text{m}$ and also it is less dispersive (see for example the dashed curve). Concentrating towards the $\text{Im}\chi_{xxxx}^{(3)}(-\omega; -\omega, \omega, \omega)$ the first peak which is obviously a two-photon absorption one which is exactly at the same photon energy as the second peak of Fig 1 (a). This conclusively proves that the second peak is a two-photon one in agreement with the explanation of experimental observation [15]. In the same spirit, the third peak of Fig 1 (c) should be a two-photon resonant one which coincides with the dip of Fig 2 (a). In contrast, in Fig. 3 (b) the dip of $\text{Im}\chi_{xxxx}^{(3)}(-\omega; 0, 0, \omega)$ is exactly at

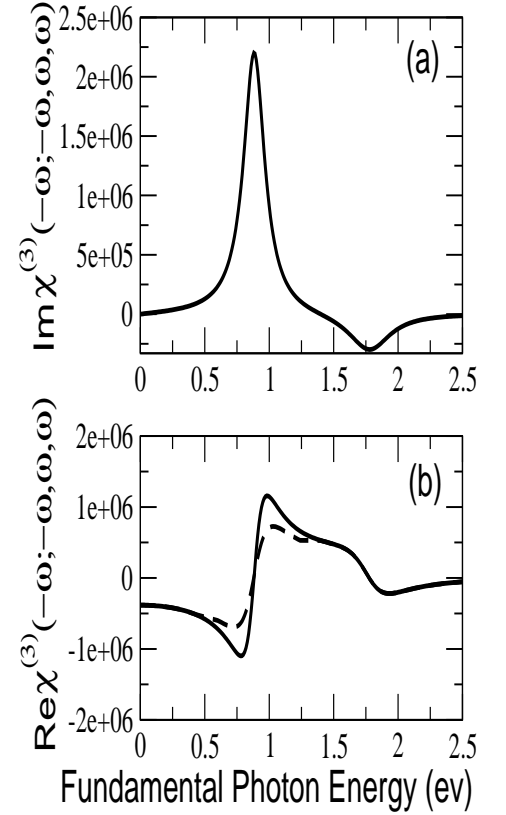


FIG. 2: Theoretical prediction of third order susceptibility of one dimensional Mott-Hubbard insulators relevant for two-photon absorption (TPA) as well as intensity dependent refractive index (n_2). The panel (a) represents imaginary part of the third order susceptibility whereas (b) the real part. Both the real and imaginary parts show peaked structure around 0.88 eV (optical fibre communication length). The dashed curve in (b) corresponds to the case of higher value of linewidth parameter $\Gamma_a = 0.4$ eV compared to the solid line case, $\Gamma_a = 0.3$ eV.

the double that of the second peak (ω_B) in Fig. 1 (a) in accordance with the experimental observations (see for example Fig. 2(e), (f) of [15]). Thus in order to observe the higher energy two photon state one should measure the $\text{Im}\chi_{xxxx}^{(3)}(-\omega; -\omega, \omega, \omega)$ and a signature of the higher energy peak is perhaps already there in the experimental observation (see for example Fig. 1(c) of [15]).

The Im $\chi_{xxxx}^{(3)}(-\omega, 0, 0, \omega)$ is related to electro absorption (EA). A look to the expression in Eqn. (6) indicates that it would show two-photon resonant states with resonance to ω . Thus the dip in Fig. 3 (b) actually cor-

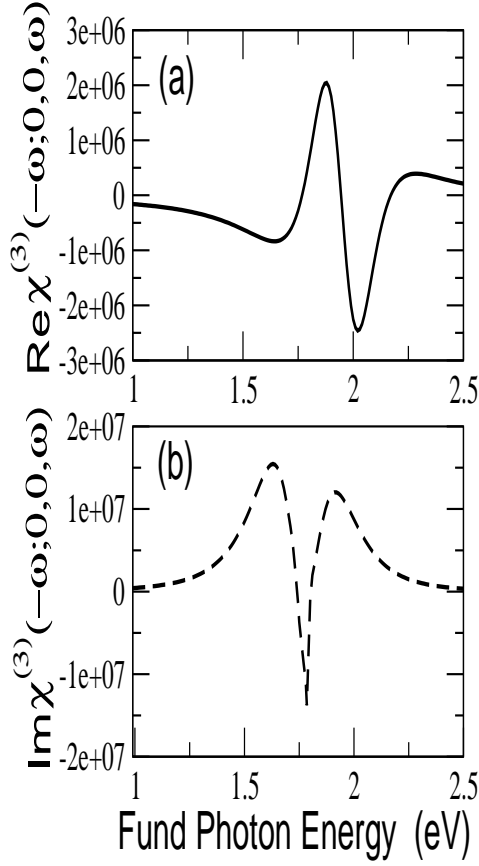


FIG. 3: Nature of real (a) and imaginary (b) parts of third order susceptibility $\chi_{xxxx}^{(3)}(-\omega, 0, 0, \omega)$ in arbitrary units as a function of fundamental photon energy (in eV). The $\text{Im} \chi_{xxxx}^{(3)}(-\omega, 0, 0, \omega)$ is related to electro absorption (EA). The dip at around 1.77 eV in the EA spectra corresponds to the two-photon resonant peak seen at ω_B in the THG spectra.

responds to the second peak of Fig 1. (c). The $\text{Im} \chi_{xxxx}^{(3)}(-\omega, 0, 0, \omega)$ thus possibly cannot probe such higher energy peak at ω_c . Essence of all these results are summarized in Fig. 4 for convenience.

In Figure 4 (a) the magnitude of the THG susceptibility in arbitrary units is obtained as a function of fundamental photon energy. The first peak at ω_A corresponds to the three photon resonant optical state whereas the second peak at ω_B corresponds to the two photon absorption peak which is slightly higher in energy than the optical state. There is a broad higher energy two photon resonant peak at ω_C and as per the experimental findings [15] we exactly find $\omega_A \simeq 2\omega_B/3$, $\omega_C \simeq 2\omega_B$ relationship. This is due to the fact that the two-photon resonant

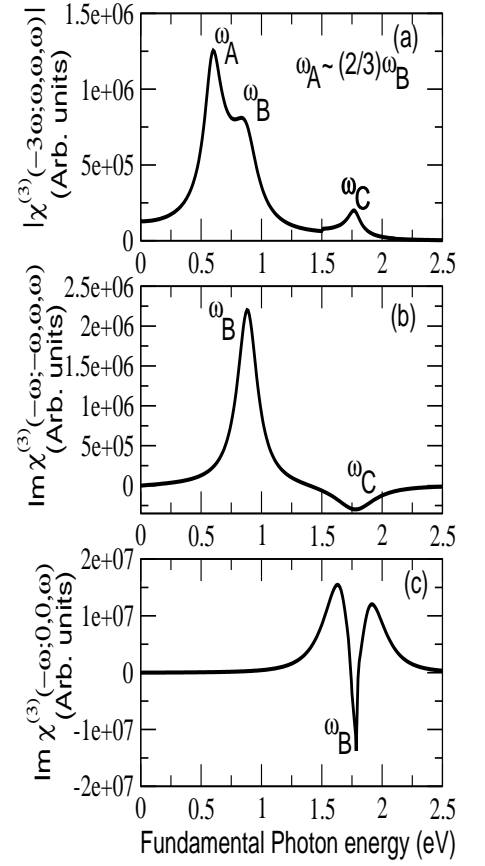


FIG. 4: Theoretical predictions of THG (a), TPA (b), EA (c). This figure conclusively proves that the third peak at ω_c is a two-photon resonant one which could be seen in the TPA spectra (b). The same should be observed in other one dimensional Mott-Hubbard systems as well.

states appear at a frequency equal to half the fundamental frequency whereas the three photon resonant ones at one third that of fundamental frequency. Thus the above relationship between ω_A and ω_B exists simply because of the fact that the first one- and two-photon state almost energetically degenerate. This does not hold in case of Ca_2CuO_3 because the two-photon state is about 0.3 eV lower in energy than the one-photon state. This is precisely the reason as to why ω_{dip} does not coincide with ω_{peak} (see Fig. 3 of [15]) in case of Ca_2CuO_3 .

In Figure 4 (b) we plot imaginary part of the third order susceptibility $\text{Im} \chi_{xxxx}^{(3)}(-\omega; \omega, -\omega, \omega)$ relevant for two photon absorption. The broad peak at ω_B in Fig. 4(a) appears exactly at the first peak of Fig. 4(b). This conclusively proves that the peak at ω_B of Figure 4(a) is

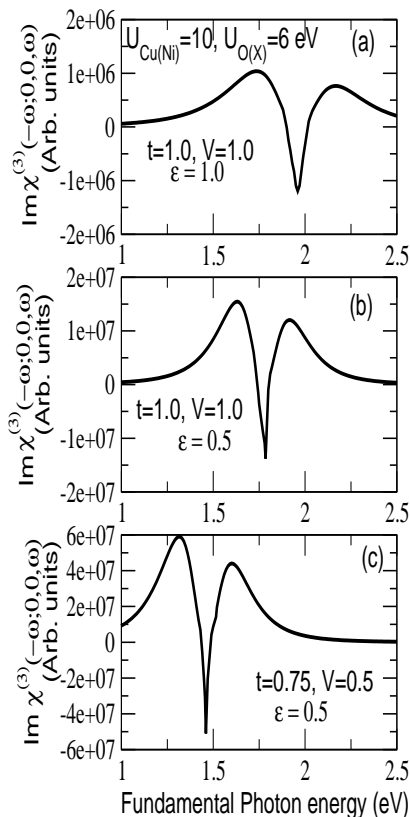


FIG. 5: Effect of lattice constant, charge transfer energy in isostructural one dimensional Mott-Hubbard insulators. For same values of on-site coulomb repulsions, in Fig (a) $\epsilon = 1.0$, $V = t = 1$ eV ; in Fig (b) $\epsilon = 0.5$ eV, $V = t = 1$ eV ; and in Fig (c) $\epsilon = 0.5$ eV $V = t = 0.75$ eV in order to simulate situation from Sr_2CuO_3 to $[\text{Ni}(\text{chxn})_2\text{Cl}]\text{Cl}_2$ to $[\text{Ni}(\text{chxn})_2\text{Br}]\text{Br}_2$.

the two photon resonant one as it appears at the same wavelength in Fig 4 (b) too. Similarly the broad peak at ω_C of Figure 4 (a) appears exactly at the dip frequency ω_c of $\text{Im } \chi_{xxxx}^{(3)}(-\omega; \omega, -\omega, \omega)$ shown in Fig. 4(b). Thus the peak at ω_C of Figure 4 (a) is also a higher energy two photon resonant absorption one [15]. We invite experimental measurements on Sr_2CuO_3 , Ca_2CuO_3 , Ni-Halide compounds of $\text{Im } \chi_{xxxx}^{(3)}(-\omega; \omega, -\omega, \omega)$ in order to verify the occurrence of higher energy even parity state.

Experimental studies on EA of one-dimensional Mott-Hubbard insulators are available in [3, 15] while the former deals with Sr_2CuO_3 and Ca_2CuO_3 compounds, the later deals with Halogen bridged Ni-halides *e.g.*, $[\text{Ni}(\text{chxn})_2\text{Cl}]\text{Cl}_2$, $[\text{Ni}(\text{chxn})_2\text{Br}]\text{Br}_2$ etc. In case of cuprates [3] only difference between the two isostruc-

tural compounds is the lattice constant which is smaller in case of Ca_2CuO_3 . This can lead to larger values of overlap between Cu-O (t_{Cu-O}) as well as intersite electron-electron repulsion (V). Considering the case of the two Ni-halide compounds mentioned above, they have difference in electro-negativity of different halides (Cl, Br) as well as difference in lattice constants [32]. Average bond distances Ni-X are different for different X ($d_{Ni-Cl} < d_{Ni-Br}$). Thus, the value of ϵ may be slightly larger in case of Cl and so the value of t_{Ni-Cl} compared to that for X=Br. The value of V should also modify accordingly (larger d_{Ni-X} smaller V). In fig. 5 we keep the values of on-site coulomb repulsions fixed for all the three cases presented (a to c) whereas the values of t , V and ϵ s are as indicated in the respective figures. More than an order-of-magnitude enhancement in the values of $\chi_{EA}^{(3)}(-\omega; 0, 0, \omega)$ is found (from Fig. 5 (a) to (c)). There is also reduction in the optical gap (from Fig. 5 (a) to (c)) in accordance with the experimental observation (see for example Fig. 2 of [3]). We find our results are in excellent agreement with the already observed data. For example, reduction in ϵ is not only sensitive to the optical gap but also enhances the nonlinearity (case of Fig. 5(a) to (b)). In case of bromide the lattice constant is also larger compared to the chloride which manifests in lower values of t as well as V . Although we have kept value of ϵ fixed in Fig 5 (b) and (c) the optical gap is reduced further to around 1.4 eV. It is conceivable that with slightly lowering the value of ϵ will reproduce the experimental optical gap 1.32 eV. We have not changed the value of ϵ in Fig 5 (b) and (c) purposefully because the effect of change in ϵ is already understood in Fig 5 (a)-(b) and the effect of ‘ t ’ to be understood. We notice that optical gap is more sensitive to the value of t than ϵ because the charge transfer energy E_{CT} is given by, $E_{CT} = \epsilon + \sqrt{\epsilon^2 + 2t^2}$. A close look to the tables I and II would indicate that the optical gap is insensitive to the values of U ’s. In correlated systems like this values of t gets renormalized [33] by electron correlation and if one uses the renormalized values of t the optical gaps obtained through exact diagonalization are reproducible via the above mentioned formula of E_{CT} . We would further like to mention that same values of U s, V are found to fit the valance-band photoemission spectra of both the Sr_2CuO_3 and Ca_2CuO_3 compounds, except the charge transfer energy — a reduced value of charge transfer energy in case of Sr_2CuO_3 [45]. This also clearly suggests lower value of ‘ t ’ in case of Sr_2CuO_3 . A further explanation to such large non-linearity may also be understood as follows. The main term dominating the spectral shape of $\chi_{xxxx}^{(3)}(-\omega; 0, 0, \omega)$ may be expressed as,

$$\frac{\chi_{xxxx}^{(3)}(-\omega; 0, 0, \omega) \propto \mu_{01}\mu_{12}\mu_{21}\mu_{10}}{(E_1 - i\Gamma_b - \omega)(E_2 - i\Gamma_a - 2\omega)(E_1 - i\Gamma_b - \omega)} \quad (7)$$

Here indices 0,1 and 2 represents respectively the ground state, one-photon allowed and two-photon allowed states. In Tables -I, II we thus tabulate the optical gap (OG) and

the product $\mu_{01}\mu_{12}$ for various parameters. With the discussions above and detailed tables we believe mechanism of optical nonlinearities is same in all the discussed 1-d Mott-Hubbard insulators and can be understood within the extended Hubbard model. Furthermore, the linewidth parameters play a strong role too, which is smallest in case of Ni-Br compounds and largest in case Ca_2CuO_3 .

In the strong correlation limit the ground state comprises of a state that contains each Cu site occupied in antiferromagnetic fashion. The lowest possible excitations are that the Cu spin moves to the left or/and right neighbouring O. The lowest one photon and two photon state comprises of the odd (-), even (+) combination of the above mentioned excitations which are called as odd and even charge transfer (CT) states respectively. Due to strongly correlated nature of wave functions both these states are energetically almost degenerate and this can cause very strong dipole coupling between these even and odd CT states. We come back to this point again later and show that this is the cause for gigantic enhancement in excited state nonlinearity in these classes of materials. There are higher energy excitations in which two/three of the Cu spins move to its neighbouring O. Also excitations like one of the Cu spin moves to its neighbouring O together with the neighbouring Cu spin occupies the earlier Cu (spin of which moved to the neighbouring O). The eigen state of the higher energy two photon state seen at ω_C is quite complicated but is a *even and almost equal* combinations of all the excitations mentioned above. The photoexcitation process in band insulators creates an electron-hole pair bound by their attractive coulomb interaction (Mott-Wannier exciton). The pair gives a series of bound states with odd and even parities below the gap. This is the case of silicon polymers, pt-halides, where the odd and even parity excited states are separated by energy gap as large as 1 eV which is unfavourable for large dipole moment (as it is inversely proportional to the energy difference between the pair of states). In contrast, one dimensional undoped Mott-Hubbard insulators are one hole per (Cu/Ni) site in which the ground state is antiferromagnetically ordered. In the charge excitation, the Cu hole can move to either of its left and right O, odd (-) and even (+) combination of which forms the optical state and the first two photon state respectively. Due to strong electron correlations present in these systems, the odd and even parity charge transfer states are nearly energetically degenerate and have strong dipolemoment. (Also the Cu spin can move back to it from the O with its spin flipped giving rise to spin excitation or 'spinon' which are gapless and arise close in energy to the ground state, they are optically silent (see for example [31]). Thus combined effect of confinement (one dimensionality), strong Coulomb repulsion alongwith charge transfer are responsible for huge optical nonlinearity in low dimensional Mott-Hubbard insulators. In 2-d thus one expects $- , ++, -+, +-$ symmetries since the Cu hole can also move to up and down

oxygen. $++$ has the same symmetry as the ground state. $+-$ and $-+$ are degenerate and are the optical state. The dipole coupling between the 1-ph ($+-$ and $-+$) and $++$ (2-ph) state then involves only two of the four configurations. Therefore, the transition dipolemoments between the ground and 1-ph state, as well as 1- to 2-ph state are expected to be weaker than that for 1-d and hence the non-linearities. Thus we confined our discussions only to one dimensional systems.

B. Excited state non-linear optics

So far we discussed about the ground state optical non-linear *e.g.* THG, TPA, EA processes and compared our theoretical evaluations with available experimental data. In Fig. 6 gigantic enhancement in various third order optical susceptibilities from the first 2-photon allowed state (and hence excited state nonlinearities) in comparison to that from the ground state is presented (the bare values of $\chi^{(3)}$ at very low photon energies is of the order of 10^8 in arbitrary units). It should be noted that the ground state optical nonlinearities in one dimensional strongly correlated systems are already quite large [2, 3, 9, 15] compared to other low dimensional materials. Therefore, enhancement in excited state non-linearities of the order of eight orders-of-magnitude is really remarkable. We present below a theoretical enhancement mechanism for third order nonlinear processes originating from real population of electronic excited states in strongly correlated systems. In experiments, an electronic excited state (the lowest 2-photon state in the present case) can be generated by using laser pulse at certain wavelength and then populated for time long enough to permit nonresonant measurements. Principle reasons for the enhancement of the nonlinearity from the excited state are as below. The transition energy between the first optical state and the two photon ($2A_g$) state is the smallest whereas the dipole moment between them is the strongest. Physical reason for the same are discussed in the earlier subsection. Here we would like to comment on the fact that the experimental determination of the energy difference between 1- and 2-photon states could be even smaller. This is because of the following reasons. We have provided ample evidences from theoretical as well as experimental studies [3] that the dip in the $\text{Im}\chi_{xxxx}^{(3)}(-\omega; 0, 0, \omega)$ corresponds to the location of 2-photon state whereas experimentally (see fig 2. of [3], Fig. 8 of [17]) it is indicated quite away from the same. Thus the energy difference between 1- and 2-photon states could be even smaller and energy ordering could even be reversed in accordance with [15]. It is to be noted that in their three level approximation the one-photon state is always taken below the two photon state. Although in case of cuprates they locate two photon state below one photon state whereas the reverse for the Ni-halides. The ratio of the dipolemoment between the optical state to the first two photon state in comparison to that from the ground state to the optical

TABLE I: The main contribution in $\chi_{EA}^{(3)}(-\omega; 0, 0, \omega)$ depends on the square of the product of dipolemoments between the ground state to optical (μ_{01}) and that between the optical state to the first two-photon state (μ_{12}). A correlation between the charge transfer energy, electronic correlations and non-linearity is obtained. The optical gap (OG) is found to be less sensitive to values of $U_{Cu(Ni)}$ or $U_{O(x)}$ but more sensitive to the values of ϵ and t .

ϵ	$U_{Cu(Ni)} = 10.0, U_{O(x)} = 6.0$			
	$V = 1, t = 1$		$V = 0.5, t = 0.75$	
	OG	$\mu_{01}\mu_{12}$	OG	$\mu_{01}\mu_{12}$
0.25	1.41	88	1.08	181
0.50	1.77	864	1.45	1674
0.75	2.22	125	1.91	231
1.00	2.69	59	2.38	113
1.25	3.18	41	2.78	12

TABLE II: Same as Table -I but for different values of on-site electronic correlations. For larger values of on-site electronic correlations maximum non-linearity shifts towards lower values of optical gap.

ϵ	$U_{Cu(Ni)} = 12.0, U_{O(x)} = 6.0$			
	$V = 1, t = 1$		$V = 0.5, t = 0.75$	
	OG	$\mu_{01}\mu_{12}$	OG	$\mu_{01}\mu_{12}$
0.25	1.42	142	1.08	273
0.35	1.55	260	1.22	2975
0.40	1.63	200	1.31	734
0.43	1.68	3178	1.35	412
0.45	1.72	731	1.39	317
0.5	1.81	246	1.47	197
0.75	2.26	51	1.93	59

state is an order of magnitude larger. The value of the ratio can go from 50 to 500 (see also Tables) in our calculation depending on various combinations of the parameters. For example, for a combination of the parameters ($|t| = 1.0$ eV, $U_{Cu(Ni)} = 10$ eV, $U_{O(X)} = 6$ eV, $V = 1.0$ eV, a relatively large value of line width parameter $\Gamma = 0.2$ eV) are such that the ratio is around 50. This property of the above mentioned one dimensional strongly correlated electron system is also seen experimentally (see for example Fig. 4(b) of [3]). As we mentioned earlier, due to strongly correlated nature of electronic states the odd and even CT states which are the first excited one and two photon states are almost energetically degenerate and contributes to extremely large dipole coupling between them. If one exchanges over the positions of odd and even parity states in equations (3 - 5) numerators of the optical excited state nonlinear susceptibility for THG, TPA, EA can be obtained. Since this is non-resonant process denominator may not play significant role (except at very low frequency). The maximum contribution comes from $a = c = 2$ and $b = 1$ term of the triple sums. Furthermore the ground state 0 should be replaced by $a = 2$. As a result, first optical state non-linearity can be enhanced as large as $(50)^4$ compared to that from the ground state. This is reflected in the figures 6 to 8. While Fig. 6 deals with excited state THG susceptibilities (magnitude, real and imaginary parts),

Fig 7 and 8 deals with excited state TPA and EA susceptibilities respectively. In Fig. 6 inset figures are in logarithmic scale whereas the same for Fig 7 and 8. 6 to 8 orders-of-magnitude enhancement in the terahertz frequency region whereas about three orders-of magnitude enhancement in the optical fiber communication wavelength is theoretically predicted.

In general, transition energies of $\hbar\omega_{bS_1}$ between the spin state S_1 and intermediate virtual one photon b ($b < 150$ in our study) states are all smaller than the transition energies of the S_0 ground state excitation processes. Furthermore, many excited states with large transition dipolemoments are accessible through the populated S_1 state and the S_b excited states. As it is understandable that the smaller transition energies $\hbar\omega_{ba}$ and larger transition dipolemoment of μ_{ab} cause individual excitation process that make up $\chi^{(3)}$ at the S_1 state to be larger than those of $\chi^{(3)}$ at the ground state S_0 . In addition, there are two different channels that contribute to the $\chi^{(3)}$, channel 1: $S_0 \rightarrow S_b \rightarrow S_0 \rightarrow S_b \rightarrow S_0$ where S_b is an one photon allowed excited state. This process can make negative contribution to $\chi^{(3)}$. Channel 2 : $S_0 \rightarrow S_b \rightarrow S_a \rightarrow S_b \rightarrow S_0$ where S_a is a two photon allowed excited state. In contrast to $\chi^{(3)}$ at S_0 which is dominantly channel 1 process, $\chi^{(3)}$ at S_1 is composed of a large number of terms that not only individually larger than those of $\chi^{(3)}$ at S_0 but also have a reduced degree of

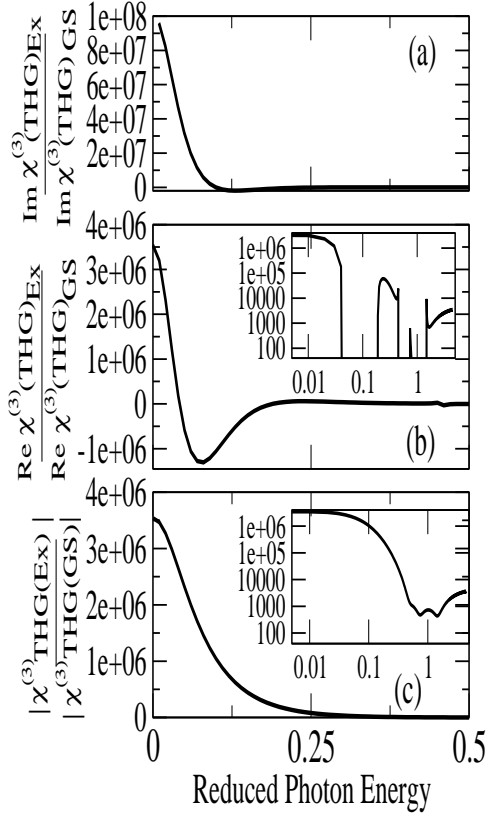


FIG. 6: Theoretical prediction of enhanced excited state nonlinearity in one dimensional Mott insulators. The panel (a) represents ratio of imaginary part of the THG susceptibility from the two-photon allowed state (EX) to that from the ground state (GS). The later is the same as that presented in Fig. 1(a). The panel (b) represents the ratio of the real part of the THG evaluated from the excited state to the ground state. The panel (c) represents the ratio of the magnitudes of the THG as indicated in the axes labels. The inset figures are indicative of the same as that of the main figure but in logarithmic scale.

cancellation effect (*i.e.*, having same sign between channel 1 and 2 processes).

C. Phenyl based π conjugated polymer

In this subsection our primary motivation is to provide explicit calculation of excited state optical nonlinearity of one of the organic systems namely PPV for direct comparison to one dimensional Mott-Hubbard systems. We study various oligomers of PPV (PPV $_n$, $n =$

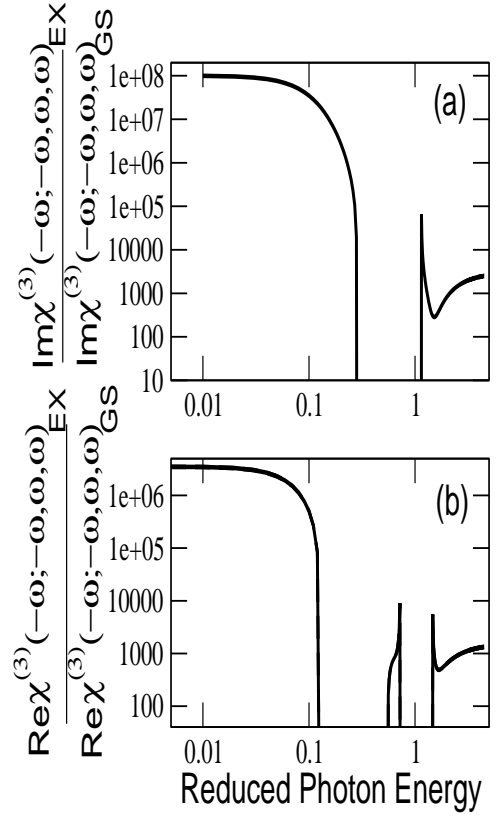


FIG. 7: Excited state enhancement of imaginary (a) and real (b) parts of the third order susceptibility with respect to the ground state relevant for TPA in logarithmic scale.

3,4,...,7) within a rigid band correlated π -electron model like Pariser-Parr-Pople (P-P-P) model Hamiltonian [34],

$$H = - \sum_{\langle ij \rangle, \sigma} t_{ij} (c_{i\sigma}^\dagger c_{j\sigma} + c_{j\sigma}^\dagger c_{i\sigma}) + U \sum_i n_{i\uparrow} n_{i\downarrow} + \sum_{i < j} V_{ij} (n_i - 1)(n_j - 1) \quad (8)$$

where $\langle ij \rangle$ implies nearest neighbors, $c_{i\sigma}^\dagger$ creates an electron of spin σ on the p_z orbital of carbon atom i , $n_{i\sigma} = c_{i\sigma}^\dagger c_{i\sigma}$ is the number of electrons with spin σ , and $n_i = \sum_{\sigma} n_{i\sigma}$ is the total number of electrons on atom i . The parameters U and V_{ij} are the on-site and long-range Coulomb repulsions, respectively, while t_{ij} is the nearest neighbor one-electron hopping matrix element that includes bond alternation and connectivity. The bond alternation appears due to electron-phonon interaction when treated in SSH [35] fashion. The parametrization of the intersite Coulomb interactions is done in a manner

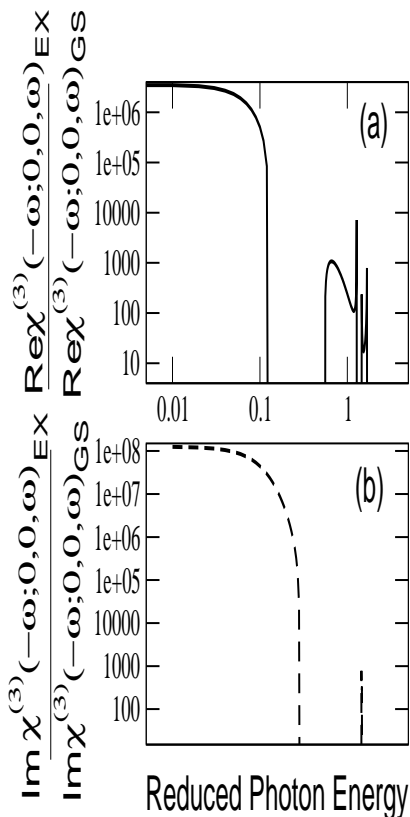


FIG. 8: Excited state enhancement of real (a) and imaginary (b) parts of the third order susceptibility with respect to the ground state relevant for EA in logarithmic scale.

similar to the Ohno parametrization [36]

$$V_{i,j} = U/\kappa(1 + 0.6117R_{i,j}^2)^{1/2}, \quad (9)$$

where κ is a parameter which has been introduced to account for the possible screening of the Coulomb interactions in the system [37–39]. We have examined both the standard Ohno parameters ($U = 11.13$ eV, $\kappa = 1.0$), as well as a particular combination of U and κ ($U = 8.0$ eV, $\kappa = 2.0$) that was found previously to be satisfactory at a semiquantitative level for explaining the full wavelength dependent ground state absorption spectrum of PPV [37, 38, 40], the latter set of values are used here, more so because the former set do not reproduce the observed PA data. We took $t = -2.4$ eV for the C – C bond in benzene rings, -2.2 eV for the vinylene linkage of the PPV oligomers single bond and -2.6 eV for the double bond. We considered PPV oligomers in their planar configurations, with the conjugation direction along the x axis. Thus the symmetry group of PPV oligomers

is C_{2h} . The two-photon states of the PPV oligomers belong to the A_g irreducible representation (irrep) of the respective symmetry group, while the one-photon states belong to the B_u irrep. The many body correlated electron calculations were achieved using the multireference singles and doubles configuration interaction (MRSDCI) approach, which is a powerful configuration interaction (CI) technique [41] that has been used previously for linear chain polyenes by Tavan and Schulten [42] as well as others [43], and by us to calculate the excited state ordering in polyphenyl- and polydiphenylacetylenes [44]. We calculate 100 excited states including the ground state *i.e.*, 50 in each subspace (A_g and B_u) and subsequently $50 \times 50 = 2500$ transition dipole moments between them for each oligomers of PPV are obtained to calculate various non-linear optical properties. Given that dimension of Hamiltonian matrices are naturally rather large (of the order of several millions) together with large numbers of dipole-moment calculations, the method is highly accurate although extremely tedious, time and space expensive.

In Fig. 9 we show the results of ground state (a) and excited state (b) THG susceptibility for PPV oligomer (6-Unit). There is more than two orders of magnitude enhancement in the excited state THG susceptibility. The enhancement magnitude does not change much with larger oligomer lengths. The ground state THG susceptibility shown in Fig. 9 (a) qualitatively agrees well with observed data [44]. We would like to further mention that similar calculations for π -conjugated polymers like trans-polyacetylene (t-PA) has also been performed through highly accurate quantum chemistry method called multireference single double configuration interaction [29, 30] and one can expect excited state (optical) nonlinearity by about two orders of magnitude in comparison to that from the ground state (details of which would be reported elsewhere). Thus superiority of one dimensional Mott-Hubbard insulators over π -conjugated organic materials as far as excited state non-linearities are concerned is established.

V. SUMMARY AND CONCLUSIONS

The realization of all-optical switching, modulating and computing devices is an important goal in modern optical technology. Nonlinear optical materials with large third-order nonlinear susceptibilities, fast response time, low loss and operability at room temperature are indispensable for such devices, because the magnitude of this quantity strongly influences on the instrument performance. Large optical nonlinearity and subpicosecond recovery are known in organic materials [25, 26] but further improvement in sample quality and morphology is required for actual application. The strongly correlated one dimensional Mott insulators like Sr_2CuO_3 , Ca_2CuO_3 on the one hand possess large non-linearity, ultrafast recovery time comparable to organics, superior thermal

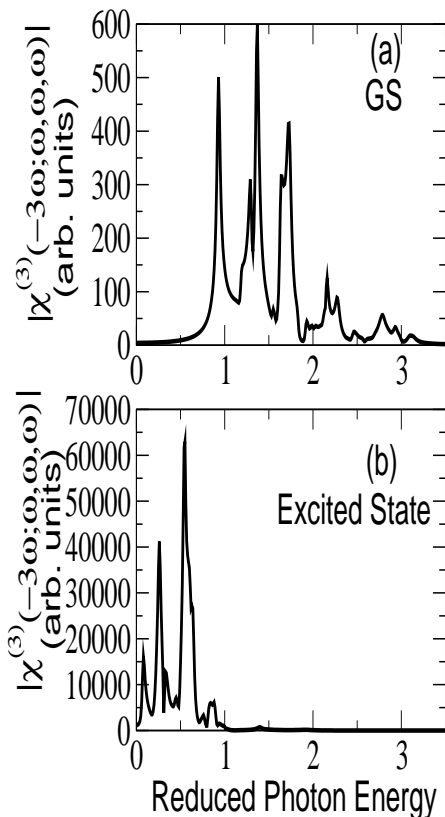


FIG. 9: Third harmonic generation (THG) susceptibility (a), excited state THG susceptibility (b) for poly-(paraphenylenevinylene) (PPV).

conductivity and higher damage threshold of inorganics [2, 9]. This along with such a huge enhancement in the excited state nonlinearity would perhaps make these materials appropriate for all optical switch devices. Until recently, the terahertz (THz = $10^{12}Hz$) region of the electromagnetic spectrum from about 100 GHz to 10 THz has been almost inaccessible because of lack of efficient sources and detectors in this THz gap. A detailed discussion of the THz sources, coherent detectors, and modulators are given in [27]. THz communication is in the very early stages of development, with first data transmission in this frequency range recently reported [28]. The THz regime is $1THz = 33.3cm^{-1}$ (wavenumber) = $300\mu m$ (wavelength) = $4.1meV$ (in comparison optical fiber communication wavelength is $1.55\mu m = 0.8 eV$). In Figs. 6–8 we have shown the excited state enhancement in nonlinearities in the lower frequency regime (longer wavelength) relevant for THz and intermediate frequency regime and optical fiber communi-

tions regime respectively. It is evident from the Figs. 6–8 that in the THz communication region the optical nonlinearity is several orders-of-magnitude larger – *which may not be possible to achieve* from ground state. Therefore we hope that the one dimensional strongly correlated systems like Sr_2CuO_3 , Ca_2CuO_3 etc. may be usable as non-linear optical medium suitable for THz communication by actually populating the first two-photon state sufficiently long enough time such that the system can be operated for nonresonant nonlinear process.

We have discussed in detail the origin of gaint ground and excited nonlinear optical properties in low dimensional Mott-Hubbard insulators. We have theoretically demonstrated the observed THG spectrum and that the *oscillatory structure* at ω_C is another higher energy two-photon state which may be verified experimentally. We also presented TPA, EA theoretically and compare with available experimental data. These results of ground state non-linear as well as linear properties compare excellently well with experiments. Then we considered the case of third-order nonlinear optical susceptibilities from an excited state rather than the ground state. We predict from our theoretical calculation that these classes of materials would have *several orders-of-magnitude larger* excited state optical nonlinearities (*e.g*, excited state-THG, -TPA, -EA) compared to that from the ground state in the THz frequency regime. Theoretically (as well as from already known experimental data) we emphasis this is an artifact of strongly correlated nature of these systems — π -conjugated polymers can also have about two orders of magnitude larger excited state optical nonlinearity compared to that of the ground state. So far it was well known that π -conjugated organic molecules and polymer systems are of interest due to the delocalized π -electron systems which give rise to large values of $\chi^{(3)}$ but one dimensional Mott-Hubbard systems on the contrary are not so delocalized but dominated by electron-electron repulsion. We pointed out discrepancies in earlier experimental studies as far as energy orderings of lowest 1- and 2-photon states are concerned. We pointed out its immense significance as far as excited state nonlinearities are concerned. For example, one can populate the optical state with appropriate excitation which would be depopulated to the lowest 2-photon state at ultrashort time and would stay their for sufficient time because it is dipolly forbidden to the ground state. (This seems to the actual case for cuprates [17]). Also excited state nonlinearity dependence on the degree of population of the concerned excited state. Since the two electronic one and two-photon states are energetically degenerate, direct jump from the one-photon state to the lower two photon state may be expected from the cuprates, which *would* emit THz radiations. Thus cuprates could be great THz radiation source — must be experimentally verified. For a case study of Ca_2CuO_3 negative photoinduced absorption (PA) was predicted [31]. Furthermore, choice of large optical non-linear medium depends not only on the ground state but also the excited states matter [20].

Finally, we have studied and solved finite size [46] one dimensional extended Hubbard model exactly to model one dimensional strongly correlated systems. We showed that the calculated THG spectrum reproduces exceptionally well the experimentally observed one. We pointed out that there exists a higher energy two photon state which can be experimentally verified. Most importantly we showed that these materials would be potential candidate for next generation on chip Thz communication for which excited state nonlinearity is essential. This is because of *unique* strongly correlated nature of these systems which makes the lowest CT one-photon and two-photon states almost energetically overlapping and very large dipole coupling between them. Like electron-electron correlation has modified many fundamental notions of superconductivity (*e.g.* High- T_c superconductivity compared to BCS), Magnetism (compared to band magnetism), Metal-Insulator transition, application of these materials for on chip Thz communication, all optical switching devices would perhaps bring a new era in optics too.

The author thanks Dr. S. C. Mehendale, S. Mazumdar, A. Shukla for useful discussion. The author also thanks Dr. Rama Chari for useful discussions, comments on Thz on chip communications. The author also thanks Max Planck Institute for complex systems, Dresden, Germany for financial support.

-
- [1] P. W. Anderson, Nature, **235** (1987) 1196 ; S. R. Julian, C. Pfleiderer, F.M. Grosche, N.D. Mathur, G.J. McMullan, A.J. Diver, I.R. Walker and G.G. Lonzarich, J. Phys. - Condens. Matt. **8** 9675-9688 (1996).
- [2] T. Ogasawara, M. Ashida, N. Motoyama, H. Eisaki, S. Uchida, Y. Tokura, H. Ghosh, A. Shukla, S. Mazumdar and M. Kuwata-Gonokami, Phys. Rev. Lett. **85**, 2204 (2000).
- [3] H. Kishida, H. Matsuzaki, H. Okamoto, T. Manabe, M. Yamashita, Y. Taguchi and Y. Tokura, Nature (London) **405**, 929 (2000).
- [4] Y. Mizuno, K. Tsutsui, T. Tohyama and S. Maekawa, Phys. Rev. B **62**, R4769-R4773 (2000).
- [5] G. P. Zhang, Phys. Rev. Lett. **86**, 2086 (2000).
- [6] C. Kim, J Electron Spect. **117**, 503 (2001). Sadamichi Maekawa and Takami Tohyama, Rep. Prog. Phys. **64**, 383 (2001).
- [7] Akira Takahashi, Hiroki Gomi and Masaki Aihara, Phys. Rev. B **69** 075116 (2004).
- [8] I. A. Zaliznyak, H. Woo, T. G. Perring, C. L. Broholm, C. D. Frost and H. Takagi, Phys. Rev. Lett. **93**, 087202 (2004)
- [9] M. Ashida, T. Ogasawara, Y. Tokura, S. Uchida, S. Mazumdar, M. Kuwata-Gonokami, Applied Phys. Lett. **78**, 2831 (2001).
- [10] S. Iwai, M. Ono, A. Maeda, H. Matsuzaki, H. Kishida, H. Okamoto and Y. Tokura, Phys. Rev. Lett. **91**, 057401 (2003).
- [11] A. S. Moskvina, J. Mlek, M. Knupfer, R. Neudert, J. Fink, R. Hayn, S.-L. Drechsler, N. Motoyama, H. Eisaki and S. Uchida, Phys. Rev. Lett. **91**, 037001 (2003).
- [12] M. Ashida, T. Ogasawara, N. Motoyama, H. Eisaki, S. Uchida, Y. Taguchi, Y. Tokura, M. Kuwata-Gonokami, H. Ghosh, A. Shukla, and S. Mazumdar, Int. J. Mod. Phys B **15**, 3628 (2001) ; Proceedings of the international conference on *Excitonic processes in Condensed Matter EXCON 2000*, p-60 (2000).
- [13] A. Schülzgen, Y. Kawabe, E. Hanamura, A. Yamanaka, P.-A. Blanche, J. Lee, H. Sato, M. Naito, N. T. Dan, S. Uchida, Y. Tanabe, and N. Peyghambarian, Phys. Rev. Lett. **86**, 3164 - 3167 (2001). For femtosecond studies see, K. Matsuda, I. Hirabayashi, K. Kawamoto, T. Nabatame, T. Tokizaki and A. Nakamura, Phys. Rev. B **50**, 4097 - 4101 (1994); K. Matsuda Physica C **280**, 84 (1997). R. A. Kaindl, M. Woerner, T. Elsaesser, D. C. Smith, J. F. Ryan, G. Farnan, M. McCurry and G. Walmsley, Science **287**, 470 - 473 (2000); R. A. Kaindl, M. Woerner, T. Elsaesser, D. C. Smith, J. F. Ryan, G. Farnan, M. McCurry and G. Walmsley, Physica C **341-348**, 2213 - 2216 (2000). For magnetic excitations see, J. D. Perkins, J. M. Graybeal, M. A. Kastner, R. J. Birge-neau, J. P. Falck, and M. Greven, Phys. Rev. Lett. **71**, 1621 - 1624 (1993); J. Lorenzana and G. A. Sawatzky, Phys. Rev. Lett. **74**, 1867 - 1870 (1995); N. Motoyama,

- H. Eisaki, and S. Uchida, Phys. Rev. Lett. **76**, 3212 - 3215 (1996); H. Suzuura, H. Yasuhara, A. Furusaki, N. Nagaosa, and Y. Tokura, Phys. Rev. Lett. **76**, 2579 - 2582 (1996).
- [14] Makoto Takahashi, Takami Tohyama and Sadamichi Maekawa, Phys. Rev. B **66** 125102. (2002). M. Ashida, Y. Taguchi, Y. Tokura, R. T. Clay, S. Mazumdar, Yu. P. Svirko and M. Kuwata-Gonokami, Europhys Lett. **58** 455 (2002).
- [15] H. Kishida, M. Ono, K. Miura, H. Okamoto, M. Izumi, T. Manako, M. Kawasaki, Y. Taguchi, Y. Tokura, T. Tohyama, K. Tsutsui and S. Maekawa, Phys. Rev. Lett. **87**, 177401 (2001).
- [16] A. Maeda, M. Ono, H. Kishida, T. Manako, A. Sawa, M. Kawasaki, Y. Tokura and H. Okamoto, Phys. Rev. B **70**, 125117 (2004).
- [17] M. Ono, K. Miura, A. Maeda, and H. Matsuzaki, H. Kishida, Y. Taguchi, Y. Tokura, M. Yamashita, H. Okamoto, Phys. Rev. B **70**, 085101 (2004).
- [18] Q. L. Zhou, J. R. Heflin, K. Y. Wong, O. Zamani-Khamiri and A. F. Garito, Phys. Rev. A **43**, 1673 (1991); D. C Rodenberger, J. R. Heflin and A. F. Garito, Nature **359**, 309 (1992); J. R. Heflin, D. C. Rodenberger, R. F. Shi, M. Wu, N. Q. Wang, Y. M. Cai, and A. F. Garito, Phys. Rev. A **45**, R4233 - R4236 (1992) ; D. C. Rodenberger, J. R. Heflin, and A. F. Garito, Phys. Rev. A **51**, 3234 - 3245 (1995).
- [19] Lin X. Chen and D. Philip Laibale, Chem. Phys. Lett. **270**, 255 (1997).
- [20] S. R. Marder, J. W. Perry, G. Bourhill, C. B. Gorman, B. G. Tiemann, and K. Mansour, Science **261**, 186 - 189 (1993); S. R. Marder, L.-T. Cheng, B. G. Tiemann, A. C. Friedli, M. Blanchard-Desce, J. W. Perry, and J. Skindhoj, Science **263**, 511-514 (1994); S. R. Marder, C. B. Gorman, F. Meyers, J. W. Perry, G. Bourhill, J.-L. Bredas, and B. M. Pierce, Science **265**, 632-635 (1994); S. R. Marder, W. E. Torruellas, M. Blanchard-Desce, V. Ricci, G. I. Stegeman, S. Gilmour, J.-L. Brédas, J. Li, G. Bublitz, and S. G. Boxer, Science **276**, 1233 (1997).
- [21] Masatoshi Yamada, Atsushi Fujimori, Yoshinori Tokura, Rev. Mod. Phys. **70** 1039 (1998).
- [22] S. Mazumdar and Z. Soos, Synthetic Metals **1**, 77 (1979); S. N. Dixit and S. Mazumdar, Phys. Rev. B **29**, 1824 (1984).
- [23] S. Ramasesha and Krishna Das, Phys. Rev. B **42** 10682 (1990); Bhabadyuti Sinha and S. Ramasesha, Phys. Rev. B **48** 16410 (1993); S. Ramasesha, Bhabadyuti Sinha and I.D.L. Albert, Phys. Rev. B **42** 9098 (1990).
- [24] P. N. Butcher and D. Cotter, *The Elements of Nonlinear Optics*, Cambridge University Press, Cambridge, 1990.
- [25] *Nonlinear Optical Properties of Organic Molecules and Crystals*, edited by D. S. Chemla and J. Zyss (Academic, Orlando, 1987).
- [26] *Nonlinear Optical effects in Organic Polymers*, edited by J. Messier *et al.*, (Kluwer, Boston, 1988).
- [27] Michael J. Fitch and Robert Osiander, John Hopkins APL Technical Digest, **25** 2004.
- [28] T. Kleine-Ostmann, K. Pierz, G. Hein, P. Dawson *et al.*, Electron. Lett. **40** 124 (2004).
- [29] Haranath Ghosh, A. Shukla and S. Mazumdar, Phys. Rev. B **62** 12763 (2000).
- [30] A. Shukla, Haranath Ghosh and S. Mazumdar, Phys. Rev. B **67** 245203 (2003).
- [31] Haranath Ghosh, Europhys Lett. **75** (3) 468- 474 (2006).
- [32] H. Okamoto, Y. Shimada, Y. Oka, A. Chainani, T. Takahashi, H. Kitagawa and T. Mitani, K. Toriumi, K. Inoue, T. Manabe and M. Yamashita, Phys. Rev. B **54** 8438 (1996).
- [33] M. Mitra, Haranath Ghosh, S. N. Behera, Euro. Phys. Jr. B **2**, 371 (1998).
- [34] R. Pariser and R. G. Parr, J. Chem. Phys. **21** 466 (1953); J. A. Pople, Trans. Faraday Soc. **49** 1375 (1953).
- [35] A. J. Heeger, S. Kivelson, J. R. Schrieffer and W.-P. Su, Rev. Mod. Phys. **60** 781 (1988).
- [36] K. Ohno, Theor. Chim. Acta **2** 219 (1964).
- [37] M. Chandross, S. Mazumdar, M. Liess, P. A. Lane, Z. V. Vardeny, M. Hamaguchi, K. Yoshino, Phys. Rev. B **55** 1486, (1997).
- [38] M. Chandross, S. Mazumdar, S. Jeglinski, X. Wei, Z. V. Vardeny, E. W. Kwock and T. M. Miller, Phys. Rev. B **50**, 14702 (1994).
- [39] C. W. M. Castleton and W. Barford, J. Chem. Phys. **117**, 3570 (2002).
- [40] D. Guo, S. Mazumdar, S. N. Dixit, F. Kajzar, F. Jarka, Y. Kawabe and N. Peyghambarian, Phys. Rev. B **48** 1433 (1993).
- [41] R. J. Buenker and S. D. Peyerimhoff, Theor. Chim. Acta **35**, 33 (1974).
- [42] P. Tavan and K. Schulten, Phys. Rev. B **36**, 4337 (1987).
- [43] D. Beljonne, Habilitation thesis, Université de Mons-Hainaut, Belgium, (2001).
- [44] Haranath Ghosh, Chem. Phys. Lett. **426** (4-6) 431-435 (2006).
- [45] K. Maiti, D. D. Sharma, T. Mizokawa and A. Fujimori, Phys. Rev. B **57**, 1572 (1998).
- [46] Finite size effect in optical conductivity based on Hubbard model are discussed by C. A. Stafford, A. J. Millis and B. S. Shastry, Phys. Rev. B **43**, 13660 (1991). Size effects are already negligible for $N > 12$. Moreover for excited state nonlinearities we presented in terms of ratios (excited state to the ground state).